CORA Cork Open Research Archive
Cartlann Taighde Oscailte Chorcaí

Title	Pore directionality and correlation lengths of mesoporous silica channels aligned by physical epitaxy
Authors	Bolger, Ciara T.;Farrell, Richard A.;Hughes, Gareth M.;Morris, Michael A.;Petkov, Nikolay;Holmes, Justin D.
Publication date	2009-07-13
Original Citation	Bolger, C. T., Farrell, R. A., Hughes, G. M., Morris, M. A., Petkov, N. and Holmes, J. D. (2009) 'Pore Directionality and Correlation Lengths of Mesoporous Silica Channels Aligned by Physical Epitaxy', ACS Nano, 3(8), pp. 2311-2319. doi: 10.1021/nn900408q
Type of publication	Article (peer-reviewed)
Link to publisher's version	https://pubs.acs.org/doi/abs/10.1021/nn900408q - 10.1021/nn900408q
Rights	© 2009 American Chemical Society. This document is the Accepted Manuscript version of a Published Work that appeared in final form in ACS Nano, copyright © American Chemical Society after peer review and technical editing by the publisher. To access the final edited and published work see https://pubs.acs.org/doi/abs/10.1021/nn900408q
Download date	2026-11-14 16:25:47
Item downloaded from	https://hdl.handle.net/10468/8157

UCC
University College Cork, Ireland
Coláiste na hOllscoile Corcaigh

Pore Directionality and Correlation Lengths of Mesoporous Silica Channels Aligned by Physical Epitaxy

Ciara T. Bolger[†,ϕ], Richard A. Farrell[†,ϕ], Gareth M. Hughes[§], Michael A. Morris[†,ϕ], Nikolay Petkov[‡*] and Justin D. Holmes[†,ϕ*].

[†] Materials and Supercritical Fluid Group, Department of Chemistry and the Tyndall National Institute, University College Cork, Cork, Ireland. [ϕ] Centre for Research on Adaptive Nanostructures and Nanodevices (CRANN), Trinity College Dublin, Dublin 2, Ireland. [‡] Electron Microscopy and Analysis Facility (EMAF), Tyndall National Institute, Lee Maltings, Prospect Row, Ireland. [§] Department of Materials, University of Oxford, Parks Road, Oxford, OX1 3PH, United Kingdom.

RECEIVED DATE (to be automatically inserted after your manuscript is accepted if required according to the journal that you are submitting your paper to)

TITLE RUNNING HEAD. Pore Directionality of Mesoporous Silica Channels

*To whom correspondence should be addressed Tel: +353 (0)21 4903608; Fax, +353 (0)21 4274097; Email: j.holmes@ucc.ie or nikolay.petkov@tyndall.ie

ABSTRACT. Herein we report on the alignment of mesoporous silica, a potential host for sub-10 nm nanostructures, by controlling its deposition within patterned substrates. In depth characterisation of the correlation lengths (length of a linear porous channel), defects of the porous network (delamination), and how the silica mesopores register to the micron-sized substrate pattern was achieved by means of

novel focused ion beam (FIB) sectioning and *in-situ* SEM imaging, which to our knowledge has not previously been reported for such a system. Our findings establish that under confinement, directed deposition of the sol within channeled substrates, where the cross sectional aspect ratio of the channels approach unity, induces alignment of the mesopores along the length of the channels. The pore correlation length was found to extend beyond the micron scale, with high pore uniformity from channel to channel observed with infrequent delamination defects. Such information on pore correlation lengths and defect densities is critical for subsequent nanowire growth within the mesoporous channels, contact lay-out (electrode deposition *etc*.) and possible device architectures.

KEYWORDS pore directionality, physical epitaxy, mesoporous silica, directed self-assembly, correlation length, *in-situ* SEM imaging

BRIEFS. *In-situ* serial FIB milling/SEM imaging technique was used to evaluate pore directionality and correlation lengths of mesoporous silica thin films aligned within patterned substrates by physical epitaxy.

MANUSCRIPT TEXT.

Mesoporous silica thin films prepared through evaporation induced self assembly (EISA)[1] methods are promising candidates for a diverse range of applications including chemical sensing[2-4], nano-fluidic separation systems[5], low-*k* dielectrics[6], and host materials for nanostructures[7, 8] due to their structural regularity and porosity on the nanoscale. Unfortunately, the mesoporous structure of these films has poor in-plane translational ordering on a macro (> 1 micron) level as extended ordering is impeded by the growth of many ordered domains that are randomly orientated with respect to each other.[9] Therefore, external forces are usually required to induce long range ordering/directionality of the mesopores and enable further processing. Fabrication of uni-directional channels, either perpendicular or parallel to a substrate, would be extremely advantageous for applications such as host-guest chemistry, nano-fluidics and molecular separations. Several reports have been published over the last decade focused on developing uni-directional mesoporous channels over large areas. Techniques such

as the application of magnetic[10, 11] or electric fields[12, 13], and substrate functionalisation followed by rubbing[14, 15] have shown potential for achieving long-range uni-dimensional ordering. However, these techniques may not be CMOS compatible because although they may achieve uni-directional pores, if the pores are not aligned to identifiable markers on a larger scale further processing would be impossible, *i.e.* they may lack the necessary registration to top-down patterning methods for true device fabrication. For any alignment technique, a detailed understanding of the directionality, defect densities and correlation lengths of the pores is required to assess the method. Traditionally, transmission electron microscopy (TEM) has been used to provide two dimensional representations of samples and although such imaging offers a wealth of information, in many cases additional structural information along a third dimension is needed. For example, to investigate the propagation of defect features of the mesoporous films within the channeled substrates, and the determination of structural uniformity. Conventionally information on these properties can be provided by acquiring images of a sample from a number of different orientations or by applying TEM tomography.[16] Alternatively, FIB milling combined with SEM imaging to produce a sequential series of cross sections (serial sectioning) has been used to investigate the directionality of large micron sized cracks and defects in very thick layers and monoliths.

Recently, our group has reported the influence of acute confinement on mesoporous structuring, where the alignment of nanoporous channels was affected by the use of low aspect ratio (channel width to depth) patterned Si/SiN substrates[17]. Wu *et. al* have also exploited this technique for aligning mesoporous silica films for use as resist molds.[18]. These alignment methods rely on a physically modified substrate to guide the long range order of the mesoporous silica system. Such an approach has been successfully used to control macroscopic ordering of colloidal spheres and block copolymer films.[19-21]. The technique has become increasingly useful for block copolymer systems, and as a result of the precision placement and registration imposed; devices such as FETs[22] and magnetic media[23] have all benefited from this technique. Whereas block copolymer films have the tendency to migrate into a trench as a result of capillary forces during thermal or solvent annealing,[24] the same cannot be said for

mesoporous oxides because of the rigidity of the silica framework. Hence post-processing steps for the removal of unwanted mesoporous material on the substrate mesas, such as chemical mechanical planarisation (CMP), are needed. Moreover the previous reports by Rice *et al.* and Wu *et al.* do not consider the precise determination of pore directionality, correlation lengths of the pores or possible defect structures, the knowledge of which is crucial to the engineering of these templates for nanowire growth.

Herein we perform high resolution serial FIB-milling/SEM sectioning along the length of mesoporous channels deposited within the channels of patterned substrates. We used optimized FIB milling conditions (low Ga-ion dosages with electron and ion beam deposited protective layers) which provide realistic information on the correlation length, uniformity and defect density of the channeled mesoporous structures. Additionally the mesoporous structures were examined by TEM as thin sections from a number of different orientations with respect to the long axis of the confining trenches. Dip coating the substrate with the sol in the direction of the trenches in combination with precise tuning of the cross sectional aspect ratio of the trench (base width to channel depth) influences the templating process and induces alignment of the mesopores to several microns in length. Additionally the mechanical stress associated with the template removal (calcination) for films deposited within substrate channels is significantly different to films deposited on planar substrates and results in considerable perturbation of the mesophase structure forming concave lattice planes.

Results and Discussion

Mesophase structure within patterned substrates. Herein optimized silica/Pluronic 123/ethanol sol-gel systems were used to coat planar and patterned silicon substrates by dip and spin coating methods. The depositions were performed at a spin coating speed of 3000 rpm or a dip coating speed of 60 mm min^{-1}, at a humidity of 70 %, resulting in highly textured mesoporous silica films with a thicknesses between 70-80 nm on a planar substrate (see Figure 1, top-down and cross sectional TEM images of planar films). The observed structure of the films is contracted *p6mm* with the mesopores adopting

excellent ordering in the direction perpendicular to the substrate plane, but with poor in-plane alignment (Figure 1).[25] For the P123 system and conditions used, at a concentration of ~40 wt% and 60 °C, the formation of this *p6mm* structure is well established. The entropically unfavourable overlap of ethylene oxide groups results in aggregate formation for all Pluronic based triblock copolymers. Growth of these aggregates at a temperature above 25 °C results in hexagonally ordered cylinders as the most stable phase.[26]

The structures deposited within patterned silicon substrates showed a remarkable difference in their final mesostructure depending on the deposition method used, *i.e.* spin versus dip coating. Figures 2 (a) and (b) show cross-sectional TEM images of the mesoporous films taken in the direction parallel to the long axis of the trenches. These images highlight the difference in structure between films deposited by spin and dip coating techniques, at a constant humidity of 70 %, and at equivalent sol-gel concentrations (the standard concentration). Mesostructures fabricated on patterned substrates *via* dip coating reveal the presence of a well ordered porous system whereby the trench has a strong effect on the alignment of the mesoporous channels. In contrast, mesostructures deposited by spin coating were less ordered and the influence of the trench was barely discernible. The difference in ordering of the mesopores for the spin *vs* dip coating processes is thought to be due to the flow of the sol in each case. Directional flow of the sol is brought about by the dip coating process which cannot occur during spin coating. Similar dip-coating experiments within channeled substrates were carried out by Wu *et al.* The authors concluded that since the air/liquid and liquid/substrate interfaces act as order fronts during EISA, deposition within a trench involves two additional liquid/substrate interfaces, *i.e.* the channel side walls.[18] During directed deposition the sol-gel interacts with all three surfaces. Templated mesophase structuring is well known to form hexagonal arrays of cylinders oriented parallel to the substrate surface.[27] It is therefore reasonable that the sol-gel interacts with all three channel surfaces such that the final mesophase contains cylinders with the C-axes parallel to the channel base and sidewall. In addition, the flow of the sol in the direction of the channels (during dip-coating) also introduces a shearing force in this direction which may favor cylinder assembly along the channel length. Experiments at different spin coating rates

and concentrations of the deposition sol showed very poor or no structural ordering. Thus we also suggest that the spin coated films within trenches lack structural direction due to the non-uniform surface of the patterned substrate.

Notably, the difference in the mesophase structure for the spin and dip coated films was not evident in the reflection XRD experiments. Films deposited by spin and dip coating, on both planar and patterned substrates (see Supporting Information, Figure S1) showed only one relatively broad reflection with no second order signals. This is not surprising since the geometry of the reflection XRD experiment allows for detection of structural information only from planes oriented parallel to the substrate surface. Such planes would be present in films deposited on both planar and patterned substrates. Although the TEM investigation confirmed poor structural ordering for the spin coated patterned substrates, the XRD signal can be a result of scattering from disordered mesoporous domains with the same critical dimensions as those for the well textured films. Notably conventional reflection XRD is not sensitive to the detection of in-plane alignment and as such, may serve only as an indication of the existence or lack of mesostructured ordering in the films. In previous reports grazing incidence XRD measurements were used to explore uni-directional mesopore alignment[14,18]. This technique relies on the disappearance of the signal scattered from the (110) set of planes of the 2 D hexagonal phase which are oriented perpendicular to the substrate plane. Nevertheless it is not sensitive to local defects or the existence of grain boundaries and cannot be used to extract pore directionality on the nanometre scale. The observation of the uni-directional alignment of mesopores within the channels only when the substrate is dip coated along the direction of the trenches agrees well with early work by Trau *et al.*, where directed liquid flow by micro-moulding in capillaries (MIMIC) was used to align mesoporous silica [12]. On the contrary, Wu *et al.* showed alignment of mesoporous silica in resist trenches when the films were deposited by spin coating from a sol-gel mixture that formed considerable overfilling of the trenches [18].

Influence of the trench size and the concentration of the coating sol. Further analysis of the films by TEM within the patterned substrates sliced in different directions was performed only with the films deposited on patterned substrates by dip coating. These substrates were selected because coating in the

direction of the trenches revealed well ordered structures with the potential for one directional alignment. Figures 2 (e) and (f) display cross-sectional TEM images of the sample shown in Figure 2 (a). The structures were imaged perpendicular to the long axis of the trench as indicated with arrows in Figure 2 (a). The images in Figure 2 (a), (e) and (f) suggest that the mesophase films within the channels are well aligned with the side walls of the trench, forming mono-domain structures. Based on the TEM measurements, correlation lengths of 300 to 500 nm were determined for that particular sample. Images of similar structures reported in previous publications by Wu *et al.*[18]and Rice *at al.*[17] showed mesophase structures composed of multiple domains propagating throughout the trenches, each one aligned differently with respect to the trench side walls. Furthermore, large overfilling of the trenches with excess material, observed in both cases would require additional post-processing steps for the removal of unwanted material such as chemical mechanical planarisation (CMP). Therefore, precise tuning of the deposition process to control the filling of the trenches is desirable. Figures 2 (c) and (d) confirm that such an approach is viable by controlling the concentration of the deposition mixture. For a given set of trench dimensions, simple dilution of the dip coating mixture allows for controlled deposition within the trenches to be achieved, with almost no residual structured material on the mesas (Figure 2 (c)). Moreover, the largely overfilled samples exhibit significant delamination from the side walls of the trench during calcination (Figure 2 (d)), whereas calcined samples with limited overfilling of the trenches revealed structures that were well adhered to the trench side walls. The different behavior of the materials upon calcination can be explained by the directionality of the stress dissipation during mesophase contraction and the influence of the trench side walls. The contraction of the mesophase structure in the direction normal to the substrate is well known for films on planar substrates.[9,25] A similar outcome is detected for trenches that are not overfilled (Figure 2 (c)) or which have small overfilling (Figure 2 (a)). The contraction normal to the substrate results in large perturbation of the mesophase structure, forming concave bending of the mesophase planes when in the near vicinity to the air/film and side walls/film interfaces. The sample shown in Figure 2 (d) displays no bending of the mesophase planes; hence the stress formed during calcination is dissipated by anisotropic

contraction and delamination from the trench side walls and base. In comparison to films deposited on planar substrates, the structural changes for the films within trenches showed larger perturbations of the porous network clearly imposed by the confining environment of the trench side walls. Unlike a planar substrate, here the structuring of the mesophase within the channels is confined by the existence of two additional interfaces, *i.e.* the trench side walls. These interfaces may also introduce a shear force during liquid flow and subsequent solvent evaporation, and consequently, impose a difference in the surface tension and interfacial interactions[28, 29] in comparison to the planar substrates that will substantially affect the mesophase structure. We believe that such processes can be responsible for the alignment of the mesophase channels in the initial deposition step. Subsequent template removal and contraction is also affected by the confining environment of the trench side walls and results in unusual bending of the mesophase lattice.

In order to follow the evolution of the mesophase structure in the confining environment of the trenched substrates, patterned silicon substrates with varying cross section aspect ratios (trench base to side walls ratio) were investigated. This stepwise change in the cross section of the substrate channels effectively imposes a variation in the influence of the side walls on the mesoporous structure which we believe plays a major role in the uni-directional alignment of the mesophase channels. A sol-gel mixture, of a set concentration (standard), was deposited onto patterned substrates that had five different channel cross sections, varying in aspect ratio from 10:1 to 1:3. Cross sectional TEM micrographs were taken of the thin films through the trenches to observe the local ordering and orientation of the mesoporous silica as a function of this confinement (Figure 3). The trench aspect ratio has a profound effect on the alignment of the mesopores. Very shallow trenches, with a 10:1 aspect ratio of the base to side walls, had almost no effect on the alignment of the mesopores within the channel, *i.e.* the alignment observed is comparable to a film deposited on a planar substrate (Figure 3(a)). Increasing the depth of the trenches to aspect ratios of 3:1 showed some pore alignment within the trenches, nucleated at the trench corners (Figure 3 (b)). Since the strength of the confining effect is expected to be the largest at these regions it is not surprising that the alignment starts here first.[29-31]

A further decrease in the aspect ratio of the trenches to 1:1 resulted in full alignment of the mesophase channels along the trench base and side walls (Figure 3 (c)). As mentioned, the deposition process can be tuned in terms of the concentration of the sol and the channel dimensions of the substrate used to control the filling. For example, when the mesoporous films were deposited within trenches with an aspect ratio of 3:1 using more dilute coating mixture (relative to standard concentration) almost fully aligned channels were observed with no material on the mesas (Figure 2 (c)). Note that all deposition mixtures used throughout the study exhibited similar viscosities that were not much different than the viscosity of the solvent due to the high dilution.

Figure 3 (d) shows the effect of imposing extreme confinement on a film, where a trenched substrate with a cross sectional aspect ratio of 1:4 was used. The orientation of the channels changed almost completely from parallel to perpendicular to the base of the trench (parallel to the side walls) compared to films deposited on a planar substrate or channeled substrates with higher channel cross sectional ratios. Only a small amount of the mesoporous material, which was in close vicinity to the trench base and air/liquid interface preserved its parallel orientation. When the deposition was performed within trenches with vary narrow and curved shapes (Figure 3(e)) the structure of the material was considerably perturbed forming curved mesophase planes. Such structures are under considerable stress during deposition and subsequent calcination due to the extreme confinement imposed by the reduced dimensions of the trenches.

Deposition within metal trenches. Additionally, we explored mesoporous silica films deposited between aluminum lines capped with silicon oxy-nitride (Figure 4). Integration of such nano-sized porous oxides between metal interconnects is highly desirable for ultra low-*k* isolation in back-end silicon chip manufacturing. The cross sectional aspect ratio of the metal trenches was set to 2:3 and the depositions were performed by dip coating along the trenches from a sol-gel mixture with standard dilution. Well textured and aligned films are formed between the metal lines, which confirms the influence of the cross sectional dimensions of the trenches. An aspect ratio of 2:3 is evidently close enough to 1:1 to induce alignment along the length similarly to that observed with the channeled silicon

substrate in figure 2c. The mesoporous structure was also contracted, forming bent planes close to the air/film interface, similarly to the films deposited within channeled silicon substrates. Interestingly the mesoporous structure was well adhered to the metal lines and delaminated from the silica base of the trenches.

In-situ serial FIB milling/SEM imaging. Although cross sectional TEM micrographs reveal a wealth of information on pore size, ordering and orientation of the mesoporous channels, the long range directionality and the length of the aligned pores can only be obtained by introducing an additional dimension in the imaging. Here we use serial FIB sectioning and direct imaging of the pores within the channels to obtain information on the pore size, ordering and orientation. Plan view SEM cross-sectional images of the metal lines and incorporated mesoporous films are shown in Figure 4 (a) and (b). A thin layer of tungsten was first deposited on the surface by electron beam to protect the surface features of the sample, followed by a more substantial (~1 μm thick) deposition of tungsten using the ion beam (Figure 5 (c)). Not only did the tungsten provide a protective capping layer above the porous film, but a by-product of the FIB polishing processes used in the serial sectioning was the selective re-deposition of tungsten rich sputtered materials onto the internal surfaces of the newly exposed pore cross sections. This filling of the mesoporous system in turn, provided an improved contrast between the centre and the walls of the mesopores within the film for high resolution SEM imaging. In contrast, preliminary experimentation with deposited carbon protection layers did not render sufficient contrast; due to a lack of atomic number contrast between the film and the carbon materials sputtered.

The directions the structures were sectioned and imaged by SEM are displayed schematically in Figure 5 (d). Initially front-on imaging was carried out across the mesoporous silica films, which had been deposited between aluminum lines capped with silicon oxy-nitride by dip coating, such that eight neighboring trenches were sectioned. In accordance with the TEM results well structured mesoporous silica with pores orientated in the direction of the trenches are seen for each trench (see Figure 6). Some voids, as seen in Figure 6 (e) to (h), caused as a result of film delamination from the trench base and bending of the mesophase planes due to the stress associated with calcination were also detected.

Imaging of the mesophase along the diagonal and side-on directions also confirmed that mesophase channels were aligned parallel to the long axis of the trenches. Nevertheless, the structural information that can be obtained in such diagonal and side-on directional imaging is limited to several hundreds of nanometres at which the magnification is high enough to resolve the pore ordering. Accurate determination of the correlation length of the mesopores and the existence of defects in the structure on a micro-metre scale is possible through milling a series of cross sections along one trench in series and imaging at higher magnification. For this experiment, cross sections in a series were at intervals of 20 nm, with eighty-six sections in total, *i.e.* a total length of ~2 μm was sectioned and imaged. A selection of cross sectional high resolution SEM images is shown in Figure 7. The overall hexagonal structure has been seen with pores aligned along the trench is preserved for at least 2 μm. The structures were largely influenced by the existence of defects caused by delamination that results in nanoscopic voids and bending of the mesophase lattice (Figure 7 (1-4)). When the delamination was minimized, the mesophase lattice appeared well ordered and defect free. The serial sectioning carried out enabled quantification of the pore correlation lengths, which were found to be at least 2 μm. This method can be extended to larger dimensions along the trenches, however, it becomes necessary to split the experimental sectioning runs as the removal of material in the process results in the cross sectioned face being rendered out of the field of view (which must be remedied by beam shift correction or stage movement). The porous network observed in the trenches was highly uniform and had a low defect density in regions with minimal delamination. Thus the precise registration of the mesophase channels to the side walls of the trenches is limited to the regions of small or no delamination where no substantial alternation of the mesophase structure was observed. Such information is critical to understand subsequent nanowire growth, contact lay-out (electrode deposition) and possible device architectures. For example, a pore which has a correlation length of 200 nm as opposed to 2000 nm, would necessitate advanced lithography patterning capabilities in the next integration levels whereas the 2000 nm channel would not.

In summary, we performed a systematic study of the deposition parameters, sol-gel concentration and trench dimensions (aspect ratio) required to produce well-aligned mesoporous silica channels on patterned substrates. The results presented in this work have proved that directional flow of the sol-gel during dip coating onto patterned substrates, where the cross sectional aspect ratio is ~1, produces near sub-10 nm uni-directional porous channels. As previously mentioned, such films containing uni-directional pores would serve as an ideal nanostructure template to host and isolate structures on the sub-10 nm regime. Serial FIB sectioning and *in-situ* high resolution SEM imaging was used for characterization of these structures, a novel method for such a system. The correlation length was found to be at least 2 μm, and the porous network observed throughout the length was highly uniform with low defects observed in the regions with minimal delamination. This FIB sectioning and *in-situ* SEM imaging technique may be extended to other porous systems once the appropriate milling conditions are established, for example block copolymers or anodised aluminium oxide (AAO) to measure similar properties (correlation length, directionality and defect density) of the pores.

Experimental Section

Silica Precursor Sol-Gel Preparation. Tetraethylorthosilicate (TEOS) was added to 0.2 M hydrochloric acid (HCl), water and ethanol (EtOH) under constant stirring in a polyethylene oxide bottle to give a final composition of TEOS 1.0/ EtOH 22/H_2O 5/HCl 0.004. This precursor solution was aged for 1 hr at 60 °C before 15 ml of Pluronic 123 (P123) block copolymer in ethanol (5 g in 100 ml solution) was added. The final silica/surfactant ratio of this standard was 5. This solution was further diluted in some cases with additional ethanol (half the volume initially added to the precursor solution) to provide control over film thickness.

Thin film Preparation. A custom-built dip coater was used to deposit the mesoporous silica thin films with the direction of withdrawal held parallel to the channels at a withdrawal rate of 60 mm min^{-1}. Films were also spin coated using a Cookson Electronics, Specialty Coating Systems, SCS G3 P-8 Spin coater at a speed of 3000 rpm (ramp rate 1000 rpm s^{-1}). Two types of patterned substrates were coated:

bare silicon substrates patterned with sub-micron scale trenches of various dimensions, and silicon substrates patterned with micron-sized aluminium grooves using a series of photolithographic, reactive ion-etching and plasma-vapour deposition steps. Planar silicon substrates were also coated as reference samples. Low angle X-ray diffraction patterns were taken of the as-deposited films with a Philips Xpert PW3719 diffractometer using Cu Kα radiation (40 kV and 35 mA) over the range $0° \leq 2\theta \leq 6°$ before and after calcination in air at 450°C for 2 hr at a ramp rate of 1 deg min^{-1}

TEM Cross Sectional Imaging. Cross sectional sample preparation was performed on thin films deposited on planar and patterned silicon substrates using a Gatan cross-sectional TEM specimen preparation procedure.[25] Briefly, a Gatan ultrasonic cutter and diamond saw were used to prepare stacks containing specimens of interest that were thinned by dimple grinding and finally polished by a precision Ar-ion polishing system (PIPS). All TEM images were collected on a JEOL 2000 FX TEM operating at an accelerating voltage of 200 kV.

Focused Ion Beam (FIB) Sectioning. Serial sectioning and *in-situ* imaging of the mesoporous films deposited on the silicon substrates patterned with micron-sized aluminium grooves was carried out with a Carl Zeiss NVision 40 Cross Beam system containing a high resolution Gemini SEM and SII Zeta FIB column. A protective layer of tungsten was deposited over the region of interest in two stages; electron beam induced deposition was used to minimise surface damage prior to bulk deposition using the ion beam. Once deposition was completed, the FIB was used to a mill a wedge of 4.5 μm x 3 μm x 1.5 μm (W x H x D). A current of 700 pA was used close to the edge of the protective strip to expose the cross sectional face. This exposed face was subsequently polished back, at a lower beam current of 300 pA, to the edge of the protective layer. A polishing current of 80 pA presented a compromise between milling time and the quality of cross sectional face. The region of interested was then serial sectioned using an 80 pA beam current, after each step of polishing an image was acquired using the SEM. Each polishing step resulted in the removal of 20 nm of material from the cross section face. For each serial sectioning sequence, 30 - 50 images were acquired; it was necessary to split up longer sectioning runs due to the required magnification and consequent field of view limitations when imaging the pores. The

SEM was operated at an accelerating voltage of 20 kV with a 30 μm aperture and the in-lens secondary electron detector was used to collect the images.

ACKNOWLEDGMENT We acknowledge financial support from the Irish Research Council for Science, Engineering and Technology (IRCSET), Science Foundation Ireland (Grant 03/IN3/I375) and the ESTEEM programme for access to FIB and imaging facilities at Oxford University. We also thank Intel Ireland, and particularly Matthew Shaw, for provision of patterned substrates through the AGS project at CRANN. This research was also enabled by the Higher Education Authority Program for Research in Third Level Institutions (2007-2011) via the INSPIRE programme.

SUPPORTING INFORMATION PARAGRAPH **Supporting Information Available**. Small angle X-ray diffraction data of the deposited films. This material is available free of charge *via* the Internet at http://pubs.acs.org.

FIGURE CAPTIONS

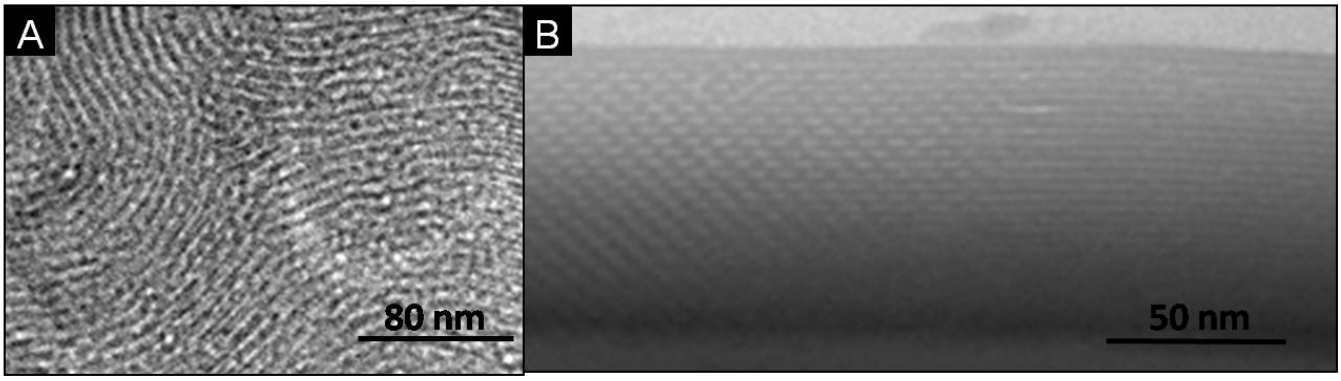


Figure 1. Top-down SEM (A) and cross-sectional TEM (B) micrographs of mesoporous thin films deposited on planar Si substrates

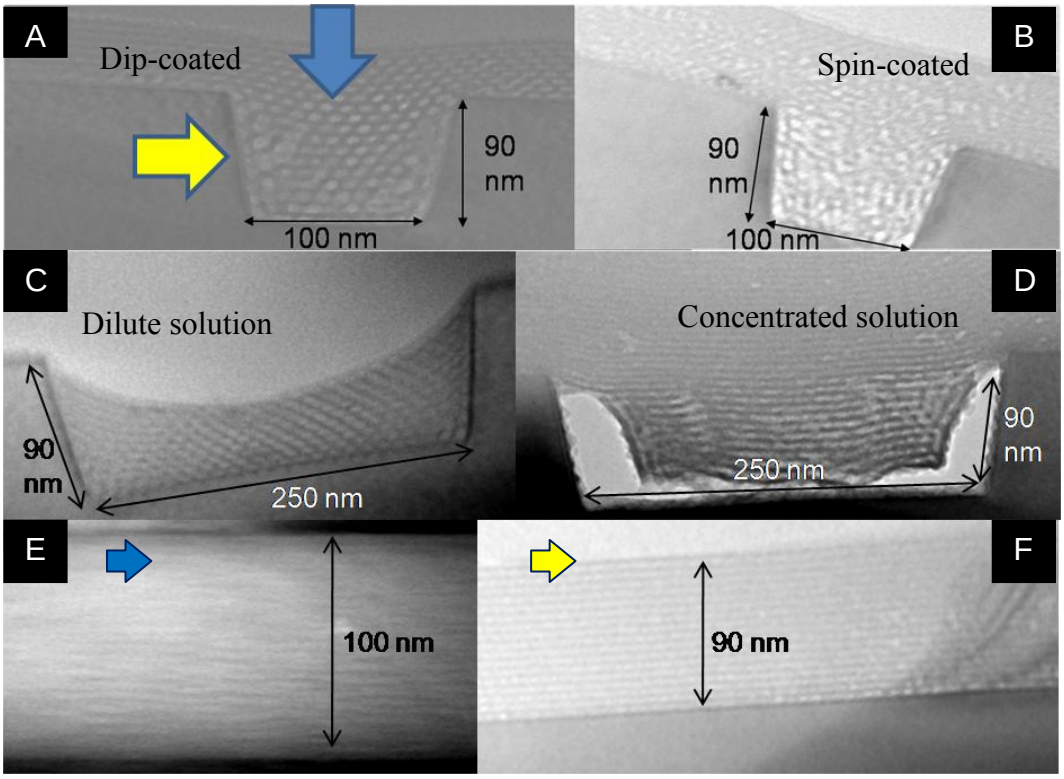


Figure 2. Cross sectional TEM micrographs of mesoporous silica deposited in channelled Si substrates: (A) dip coated, (B) spin coated, (C) using a dilute sol-gel to avoid channel overfill on to the substrate mesas, dip coated, (D) with a concentrated sol-gel showing large overfilling and severe delamination, dip coated, (E) cross sections of A along the channel length in the directions indicated by the blue arrow on image A and (F) cross sections of A along the channel length in the directions indicated by the yellow arrow on image A.

.

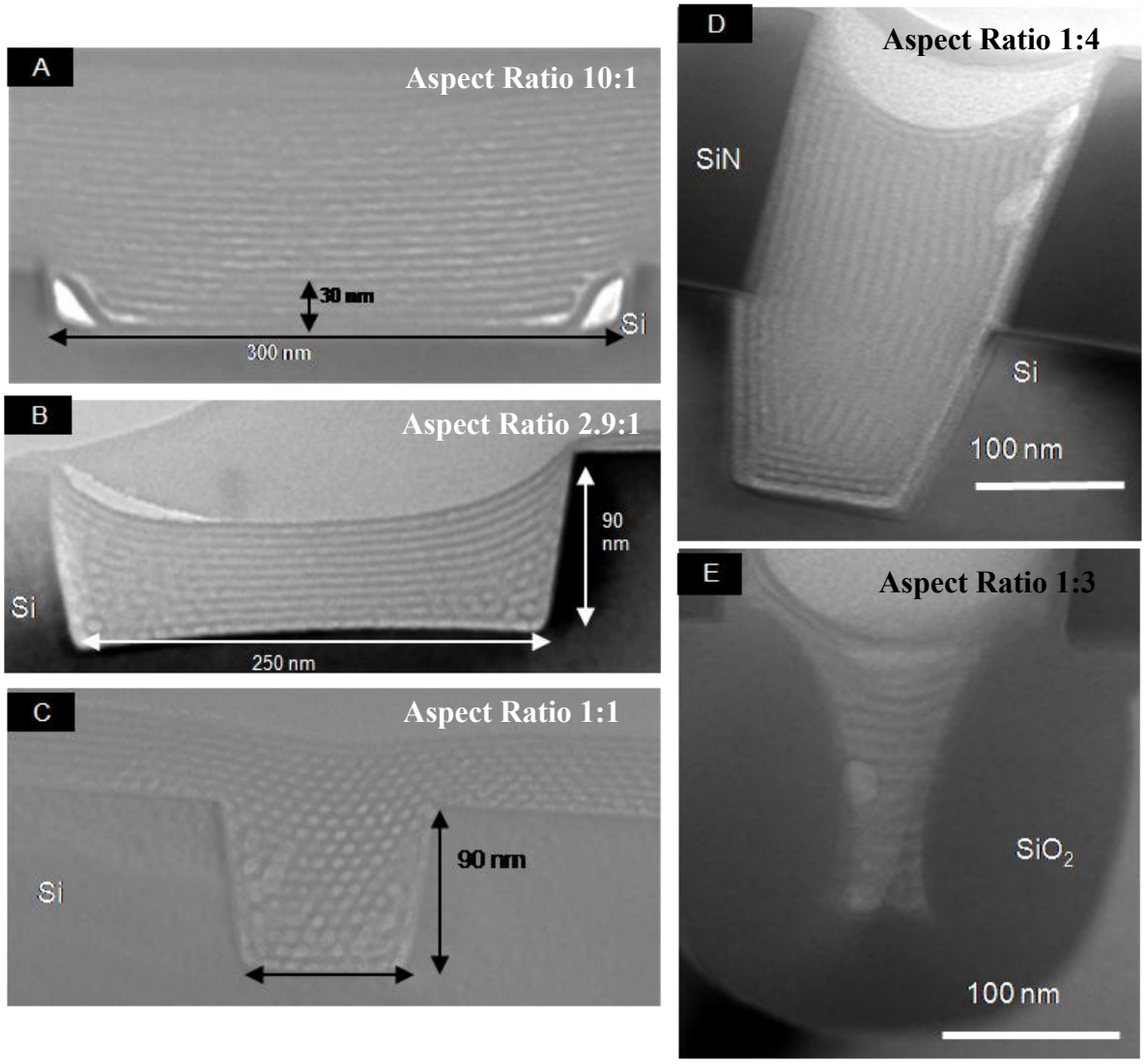


Figure 3 (A-E) Front view cross section TEM micrographs of mesoporous films within channels showing the influence of the trench cross section aspect ratio (base: sidewall lengths) on final mesostructure. To investigate extreme confinement, the oxidation of the silicon substrate used in image D was employed to reduce the trench width for image E.

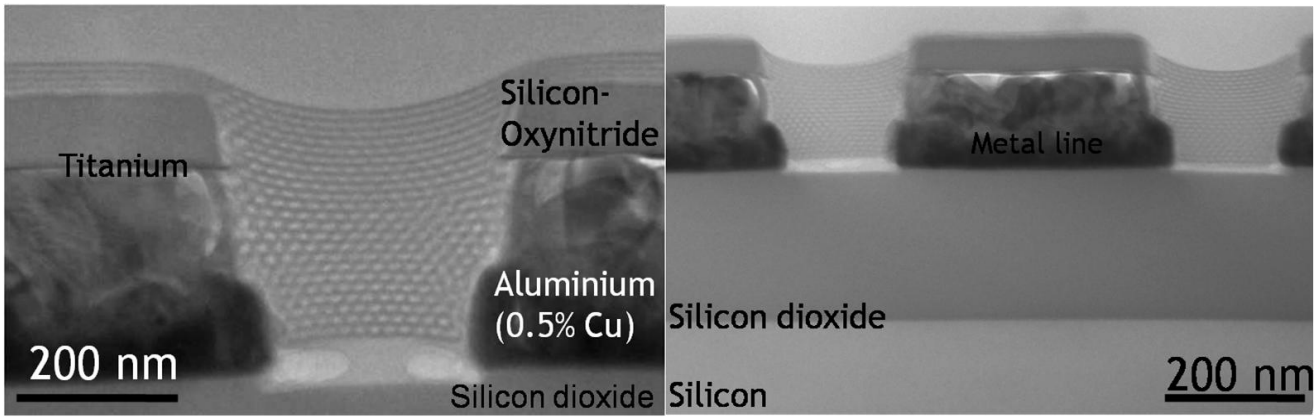


Figure 4 Cross sectional TEM micrographs of mesoporous silica confined with a patterned metal/oxide stack with an aspect ratio of 2:3.

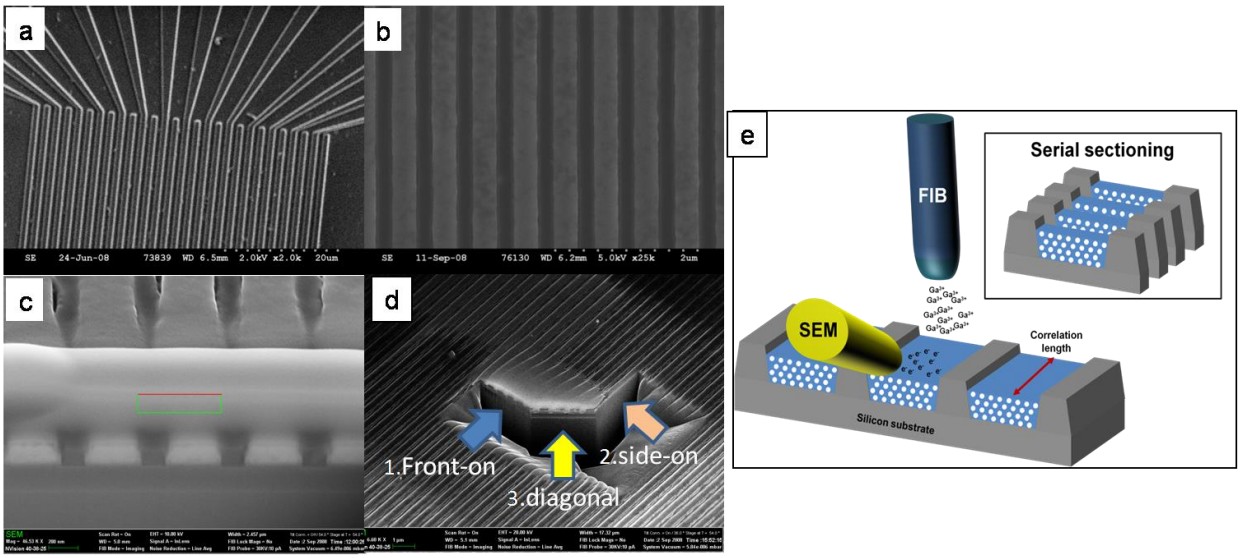


Figure 5 High-resolution SEM micrographs showing substrate patterned with aluminum lines (a), images taken at different stages during the FIB sectioning process (b-d); (b) top view SEM micrograph of mesoporous silica thin film within aluminum channels, (c) protective tungsten layer deposited on the site to be milled, (d) top view SEM micrograph of the post milled sample showing the three directions in which the SEM imaging was carried out and (e) schematic of FIB milling perpendicular to the sample and in situ SEM imaging at 54° to the sample.

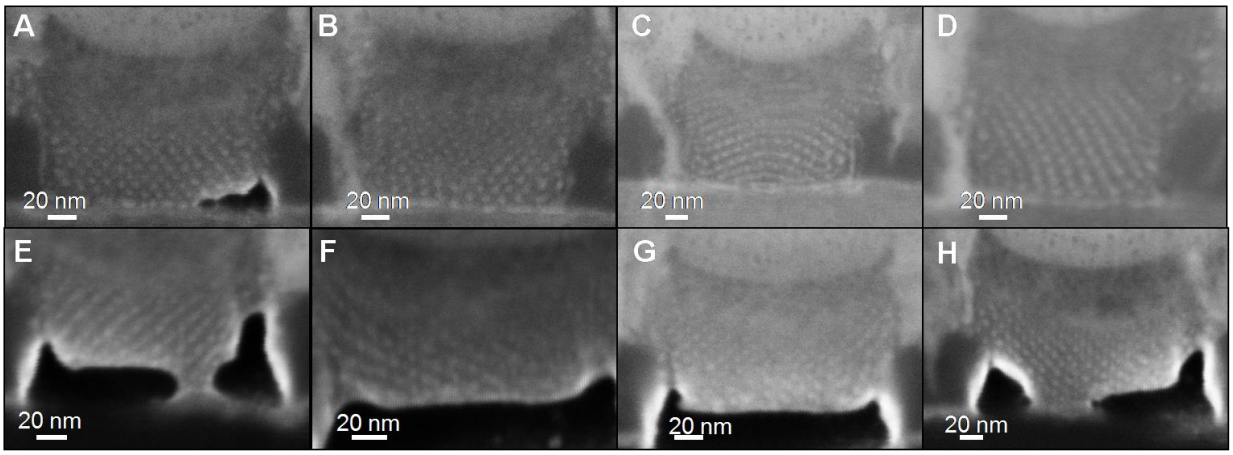


Figure 6 SEM micrographs of the 'front-on' sections taken through the mesoporous silica thin film within the channels, each showing the pore ordering of the eight separate channels (A-H)

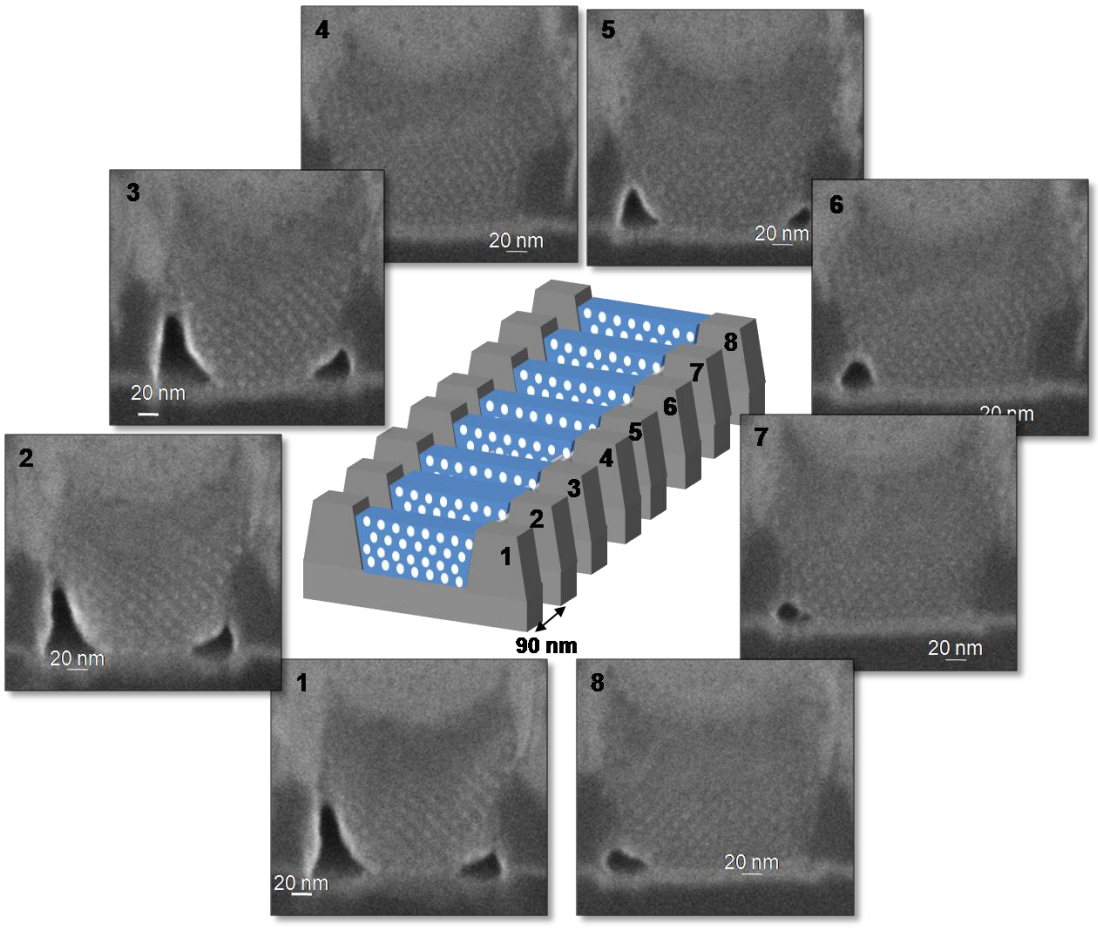


Figure 7 A selection of SEM micrographs showing exposed sections through the mesoporous silica thin film contained within a single channel. Sections shown were taken at 90 nm intervals during a serial sectioning procedure of one channel.

REFERENCES

1. Brinker, C.J. Evaporation-induced self-assembly: Functional nanostructures made easy. *Mrs Bulletin*. **2004**. *29*: 631.
2. Qi, Z.M.; Honma, I.; Zhou, H. Ordered-mesoporous-silica-thin-film-based chemical gas sensors with integrated optical polarimetric interferometry. *Appl. Phys. Lett.* . **2006**. *88*: 053503.
3. Wirnsberger, G.; Scott, B.J.; Stucky, G.D. pH Sensing with mesoporous thin films. *Chem. Commun.* . **2001**: 119.
4. Yang, C.M.; Cho, A.T.; Pan, F.M.; Tsai, T.G.; Chao, K.J. Spin-on mesoporous silica films with ultralow dielectric constants, ordered pore structures, and hydrophobic surfaces. *Adv. Mater.* **2001**. *13*: 1099.
5. Fan, H.; Lu, Y.; Stump, A.; Reed, S.T.; Baer, T.; Schunk, R.; Perez-Luna, V.; Lopez, G.P.; Brinker, C.J. Rapid prototyping of patterned functional nanostructures. *Nature* **2000**. *405*: 56.
6. Maex, K.; Baklanov, M.R.; Shamiryan, D.; Iacopi, F.; Brongersma, S.H.; Yanovitskaya, Z.S. Low dielectric constant materials for microelectronics. *J. Appl. Phys.* **2003**. *93*: 8793-8841.
7. Coleman, N.R.B.; O'Sullivan, N.; Ryan, K.M.; Crowley, T.A.; Morris, M.A.; Spalding, T.R.; Steytler, D.C.; Holmes, J.D. Synthesis and characterization of dimensionally ordered semiconductor nanowires within mesoporous silica. *J. Am. Chem. Soc.* **2001**. *123*: 7010.
8. Petkov, N.; Platschek, B.; Morris, M.A.; Holmes, J.D.; Bein, T. Oriented Growth of Metal and Semiconductor Nanostructures within Aligned Mesoporous Channels. *Chem. Mater.* . **2007**. *19*: 1376.
9. Klotz, M.; Albouy, P.A.; Ayral, A.; Menager, C.; Grosso, D.; Van der Lee, A.; Cabuil, V.; Babonneau, F.; Guizard, C. The true structure of hexagonal mesophase-templated silica films as revealed by X-ray scattering: Effects of thermal treatments and of nanoparticle seeding. *Chem. Mater.* **2000**. *12*: 1721-1728.
10. Tolbert, S.H.; Firouzi, A.; Stucky, G.D.; Chmelka, B.F. Magnetic field alignment of ordered silicate-surfactant composites and mesoporous silica. *Science*. **1997**. *278*: 264.
11. Yamauchi, Y.; Sawada, M.; Sugiyama, A.; Osaka, T.; Sakka, Y.; Kuroda, K. Magnetically induced orientation of mesochannels in 2D-hexagonal mesoporous silica films. *J. Mater. Chem.* **2006**. *16*: 3693.
12. Trau, M.; Yao, N.; Kim, E.; Xia, Y.; Whitesides, G.M.; Aksay, I.A. Microscopic patterning of orientated mesoscopic silica through guided growth. *Nature*. **1997**. *390*: 674-676.
13. Tian, B.Z.; Liu, X.Y.; Tu, B.; Yu, C.Z.; Fan, J.; Wang, L.M.; Xie, S.H.; Stucky, G.D.; Zhao, D.Y. Self-adjusted synthesis of ordered stable mesoporous minerals by acid-base pairs. *Nat. Mater.* **2003**. *2*: 159-163.
14. Miyata, H.; Kuroda, K. Alignment of mesoporous silica on a glass substrate by a rubbing method. *Chem. Mater.* **1999**. *11*: 1609.
15. Miyata, H.; Suzuki, T.; Fukuoka, A.; Sawada, T.; Watanabe, M.; Noma, T.; Takada, K.; Mukaide, T.; Kuroda, K. Silica films with a single-crystalline mesoporous structure. *Nat. Mater.* **2004**. *3*: 651.
16. de Jong, K.P.; Koster, A.J. Three-dimensional electron microscopy of mesoporous materials - Recent strides towards spatial imaging at the nanometer scale. *Chemphyschem*. **2002**. *3*: 776-+.
17. Rice, R.L.; Arnold, D.C.; Shaw, M.T.; Iacopina, D.; Quinn, A.J.; Amenitsch, H.; Holmes, J.D.; Morris, M.A. Ordered mesoporous silicate structures as potential templates for nanowire growth. *Adv. Funct. Mater.* . **2007**. *17*: 133.

18. Wu, C.W.; Ohsuna, T.; Edura, T.; Kuroda, K. Orientational control of hexagonally packed silica mesochannels in lithographically designed confined nanospaces. *Angew. Chem. Int. Edit.* **2007**. *46*: 5364.
19. Segalman, R.A.; Yokoyama, H.; Kramer, E.J. Graphoepitaxy of spherical domain block copolymer films. *Adv. Mater.* **2001**. *13*: 1152.
20. Sundrani, D.; Darling, S.B.; Sibener, S.J. Guiding polymers to perfection: Macroscopic alignment of nanoscale domains. *Nano Lett.* **2004**. *4*: 273.
21. Bita, I.; Yang, J.K.W.; Jung, Y.S.; Ross, C.A.; Thomas, E.L.; Berggren, K.K. Graphoepitaxy of self-assembled block copolymers on two-dimensional periodic patterned templates. *Science*. **2008**. *321*: 939.
22. Black, C.T. Self-aligned self assembly of multi-nanowire silicon field effect transistors. *Appl. Phys. Lett.* **2005**. *87*.
23. Cheng, J.Y.; Ross, C.A.; Chan, V.Z.H.; Thomas, E.L.; Lammertink, R.G.H.; Vancso, G.J. Formation of a cobalt magnetic dot array via block copolymer lithography. *Adv. Mater.* **2001**. *13*: 1174-+.
24. Bravman, J.C.; Sinclair, R. The Preparation of Cross-section Specimens for Transmission Electron Microscopy. *J. Electron. Micr. Tech.* **1984**. *1*: 53-61.
25. Lu, Y.F.; Ganguli, R.; Drewien, C.A.; Anderson, M.T.; Brinker, C.J.; Gong, W.L.; Guo, Y.X.; Soyez, H.; Dunn, B.; Huang, M.H.; Zink, J.I. Continuous formation of supported cubic and hexagonal mesoporous films by sol gel dip-coating. *Nature*. **1997**. *389*: 364.
26. Flodstrom, K.; Wennerstrom, H.; Alfredsson, V. Mechanism of mesoporous silica formation. A time-resolved NMR and TEM study of silica-block copolymer aggregation. *Langmuir*. **2004**. *20*: 680-688.
27. Tate, M.P.; Eggiman, B.W.; Kowalski, J.D.; Hillhouse, H.W. Order and orientation control of mesoporous silica films on conducting gold substrates formed by dip-coating and self-assembly: A grazing angle of incidence small-angle X-ray scattering and field emission scanning electron microscopy study. *Langmuir*. **2005**. *21*: 10112-10118.
28. Yang, P.; Zhao, D.; Margolese, D.I.; Chmelka, B.F.; Stucky, G.D. Generalized syntheses of large-pore mesoporous metal oxides with semicrystalline frameworks. *Nature* **1998**. *396*: 152.
29. Platschek, B.; Petkov, N.; Bein, T. Tuning the structure and orientation of hexagonally ordered mesoporous channels in anodic alumina membrane hosts: A 2D small-angle X-ray scattering study. *Angew. Chem. Int. Edit.* **2006**. *45*: 1134.
30. Alberius, P.C.A.; Frindell, K.L.; Hayward, R.C.; Kramer, E.J.; Stucky, G.D.; Chmelka, B.F. General predictive syntheses of cubic, hexagonal, and lamellar silica and titania mesostructured thin films. *Chem. Mater.* **2002**. *14*: 3284-3294.
31. Cheng, J.Y.; Mayes, A.M.; Ross, C.A. Nanostructure engineering by templated self-assembly of block copolymers. *Nat. Mater.* **2004**. *3*: 823-828.

TABLE OF CONTENTS FIGURE

